ANL-6230
Metals, Ceramics,
and Materials
(TID-4500, 16th Ed.)
AEC Research and
Development Report

ARGONNE NATIONAL LABORATORY
9700 South Cass Avenue
Argonne, Illinois

FILM GROWTH ON ALUMINUM IN HIGH-TEMPERATURE WATER

by

Raymond K. Hart and Westly E. Ruther

Metallurgy Division
Program 10.2.2

Portions of the material in this report have appeared in the
Metallurgy Division Annual Report for 1959:

ANL-5975 (95)
ANL-6099 (128, 130-131, 132)

April 1961

Operated by The University of Chicago
under
Contract W-31-109-eng-38

DISCLAIMER

This report was prepared as an account of work sponsored by an agency of the United States Government. Neither the United States Government nor any agency Thereof, nor any of their employees, makes any warranty, express or implied, or assumes any legal liability or responsibility for the accuracy, completeness, or usefulness of any information, apparatus, product, or process disclosed, or represents that its use would not infringe privately owned rights. Reference herein to any specific commercial product, process, or service by trade name, trademark, manufacturer, or otherwise does not necessarily constitute or imply its endorsement, recommendation, or favoring by the United States Government or any agency thereof. The views and opinions of authors expressed herein do not necessarily state or reflect those of the United States Government or any agency thereof.

DISCLAIMER

Portions of this document may be illegible in electronic image products. Images are produced from the best available original document.

TABLE OF CONTENTS

	Page
ABSTRACT	5
INTRODUCTION	5
EXPERIMENTAL	6
Material Used	6
Methods of Specimen Preparation	6
Testing Environments	7
Apparatus Used for Observation	7
RESULTS	7
A. Corrosion at 250°C	7
1) Aluminum	7
2) A255 alloy	10
3) X8001 alloy	14
B. Corrosion at 350°C	14
1) A255 alloy	14
2) X8001 alloy	20
DISCUSSION	23
ACKNOWLEDGEMENTS	24
REFERENCES	25

LIST OF FIGURES

No.	Title	Page
1.	Aluminum surface after 3-min corrosion in water at 250°C	8
2.	Carbon replica, preshadowed with Pt-Pd, of aluminum corroded for 4 min at 250°C	8
3.	(a) Surface topography and whisker on aluminum corroded for 10 min at 250°C. (b) Electron diffraction pattern from whisker shown in (a)	9
4.	Structure at A255 alloy	10
5.	(a) Precipitate in A255 alloy surface after 3-min corrosion at 250°C. (b) Same area as shown in (a) after 200-min corrosion	10
6.	Carbon replica, preshadowed with Pt-Pd, of A255 alloy after corrosion for 12 min at 250°C	11
7.	Carbon replica, preshadowed with Pt-Pd, of A255 alloy after corrosion for 12 min at 250°C (X16000)	12
8.	Carbon replica, preshadowed with Pt-Pd, of A255 alloy after corrosion for 12 min at 250°C (X6000)	12
9.	Outcropping on A255 alloy disc after corrosion for 4 min at 250°C	12
10.	(a) Whisker growth on A255 alloy after corrosion for 200 min at 250°C. (b) Diffraction pattern from one of these whiskers	13
11.	Outcropping on X8001 alloy disc after corrosion for 5 min at 250°C	14
12.	Outcropping on X8001 alloy disc after corrosion for 10 min at 250°C	14
13.	(a) Surface of A255 alloy after 5 min at 350°C. (b) Surface of A255 alloy after 10 min at 350°C. (c) Surface of X8001 alloy after corrosion for 200 min at 350°C	15
14.	Oxide platelet on A255 alloy disc after corrosion for 10 min at 350°C	16
15.	(a) Outcropping on A255 alloy disc after corrosion for 10 min at 350°C. (b) Diffraction pattern from the surface	17

LIST OF FIGURES

No.	Title	Page
16.	Whisker on A255 alloy after corrosion for 24 hr at 350°C. Inset is corresponding diffraction pattern	18
17.	Transverse section of an A255 alloy disc after corrosion for 32 days at 350°C	19
18.	Electron silhouette of oxide layer stripped from A255 alloy disc after corrosion for 32 days at 350°C	19
19.	Optical micrograph of an A255 alloy disc after corrosion for 32 days at 350°C	19
20.	Electron silhouette of diaspore needles protruding into the hold of the disc shown in Figure 19	20
21.	Outcropping on X8001 alloy disc after corrosion for 5 min at 350°C	21
22.	Oxide platelet on X8001 alloy disc after corrosion for 10 min at 350°C showing "loops."	21
23.	(a) Oxide particle removed from X8001 alloy disc after corrosion for 24 hours at 350°C. (b) Electron diffraction pattern from particle shown in (a)	22

LIST OF TABLES

No.	Title	Page
I.	Composition of Materials	6
II.	Whisker growth on aluminum at 250°C	13
III.	Whisker growth on aluminum at 350°C	18

FILM GROWTH ON ALUMINUM IN HIGH-TEMPERATURE WATER

by

Raymond K. Hart and Westly E. Ruther

ABSTRACT

Film growths on aluminum and two aluminum-1 w/o nickel alloys in water at 250°C and 350°C have been studied. It has been found that oxide growth does not advance on a uniform front but, to the contrary, the advancing surface contains many outcrops in the form of thin platelets, chunky outcrops, and whiskers. With both the pure metal and the alloys considerable intergranular attack was observed. The general corrosion product was usually more uniform in crystal size when formed on the pure metal, but variations in crystal size were observed on both aluminum and alloys with varying features of the metal surface. The roughness of the general oxide surface (including outcrops) was found to increase rapidly to about 0.2 micron and then remain relatively constant with increasing film thickness. The composition of films formed under all investigated conditions, except one, was found to be boehmite (α-$Al_2O_3 \cdot H_2O$). This exception was films carried by the alloy specimens after testing for 32 days at 350°C. In this case the main corrosion film was still boehmite, but in addition the outer surface supported long needles of diaspore (β-$Al_2O_3 \cdot H_2O$).

INTRODUCTION

Right from the onset of film growth on a metal surface, the topography of the oxide-free surface is very rarely smooth on a microscale, although it often appears so on a macroscale. Studies of oxidized metal surfaces by reflection electron microscopy, for instance by Halliday and Hirst,[1] have shown that these surfaces contain many irregularities which are not visible with the optical microscope. Such irregularities include undulations at grain boundaries, blistering due to entrapped gases, and various forms of outcropping.

Another method for viewing the topography of reaction products on metal surfaces is in silhouette. This method also has the advantage that in many cases the individual asperities are transparent, and so their internal structures can also be investigated. Electron microscopes incorporating selected area diffraction have proved of great benefit in these investigations.

Brenner[2] refers to observations being made on the filamentary growth of silver as early as 1877. In the intervening years between 1877 and 1950 spasmodic references can be found relating to filamentary growth of oxides, sulfides, etc. (reviewed by Nabarro and Jackson[3]). However, it was not until about 1952 that filamentary growths became a topic of intensive study. Since then these growths have been analysed by optical, electron optical, and X-ray techniques.

With particular reference to filamentary growth of aluminum oxides, Wislicenus[4] observed whisker growths of aluminum hydroxide, and Webb et al.[5,6] grew sapphire whiskers from both aluminum and $TiAl_3$.

The present paper describes the observation of various forms of outcropping on aluminum and aluminum-nickel alloys after corrosion in water at temperatures up to 350°C.

EXPERIMENTAL

Material Used:

The materials used in this study are listed in Table I.

Table I

Composition of Materials

Material	Impurities
High-purity Al	Si - 10 ppm; Fe - 10 ppm; Cu - 20 ppm; Mg - 10 ppm
A-255	High-purity Al + 1 w/o Ni + 0.1 w/o Ti
X-8001	1100 Al + 0.89 w/o Ni + 0.48 w/o Fe (0.13% Cu, 0.11% Si, 0.01% Mn and 0.02 % Ti carried by 1100 Al and not added to 1100 Al)

In each case the material was received in the form of $\frac{1}{8}$-in. thick cold-rolled sheet.

Methods of Specimen Preparation:

Two types of test specimens were used in these experiments, namely, rectangular sheets and discs. The sheet specimens were cut directly from the cold-rolled sheet and then polished either metallographically or electrolytically as desired.

Specimen discs of these materials were prepared by punching out 2.3-mm dia blanks from 0.005-in. thick foil which had been cold rolled to this thickness from $\frac{1}{8}$-in. stock. A centrally placed 0.010-in. dia hole was

drilled in each disc and, after deburring, was mechanically polished with "Wenol" metal polish on a tapered, soft wooden dowel. After the holes were smooth (determined by viewing optically at 250X), the discs were then usually given a quick electropolish in 1:9 perchloric-acetic acid bath at 60 volts, washed in isopropyl alcohol, and dried in a current of warm air. Before being used in corrosion tests, the prepared hole in each disc was viewed electron optically in silhouette at 6000X to ascertain smoothness.

Some discs were transversly sectioned after corrosion testing by mounting them in methyl methacrylate replicating plastic and mechanically grinding away layers until the desired section had been obtained.

Electron microscope specimens of oxidation products were also prepared in the following manner. Numerous $\frac{1}{32}$-in. dia holes were drilled through 0.005-in. thick foil specimens, and then the foil was corroded. At the conclusion of these tests the remaining metal was removed by dissolution in iodine-methanol as described by Pryor and Keir.[7] The freed oxide "rings" were mounted on microscope grids and viewed in silhouette.

Testing Environments

All the specimens were autoclave tested in high-purity water (1.1 to 1.5×10^6 ohm cm) at either 250°C or 350°C for times varying from a few minutes up to one month. The procedure of testing has been previously described in detail.[8] The small disc specimens were individually "caged" in platinum gauze containers while the larger specimens were suspended from artificial sapphire rods.

Apparatus Used for Observation

The corrosion products were viewed optically in both light and electron microscopes. The Siemens Elmiskop 1 employed in this investigation was fitted with an adjustable aperture located in the plane of the first intermediate image so that diffraction patterns could be obtained from selected areas.

RESULTS

A. Corrosion at 250°C

1. Aluminum

When pure aluminum is exposed to water at 250°C, the metal corrodes with great rapidity until it is totally converted to a crumbling mass of oxide. With $\frac{1}{8}$-in. thick sheet this usually happens within one day.

After only three-minute immersion, the aluminum surface showed severe intergranular attack (Fig. 1). This figure also shows what appears to be blisters adjacent to the grain boundaries. The remainder of the grains were uniformly filmed with corrosion product. Both X-ray and electron diffraction patterns showed boehmite (α-$Al_2O_3 \cdot H_2O$) to be the only material present on the surface. Figure 2 is an electron micrograph of a two-stage preshadowed carbon replica taken from near the middle of an aluminum grain. The average oxide particle size is shown to be approximately 0.5 μ, although an occasional 1-μ particle can also be seen.

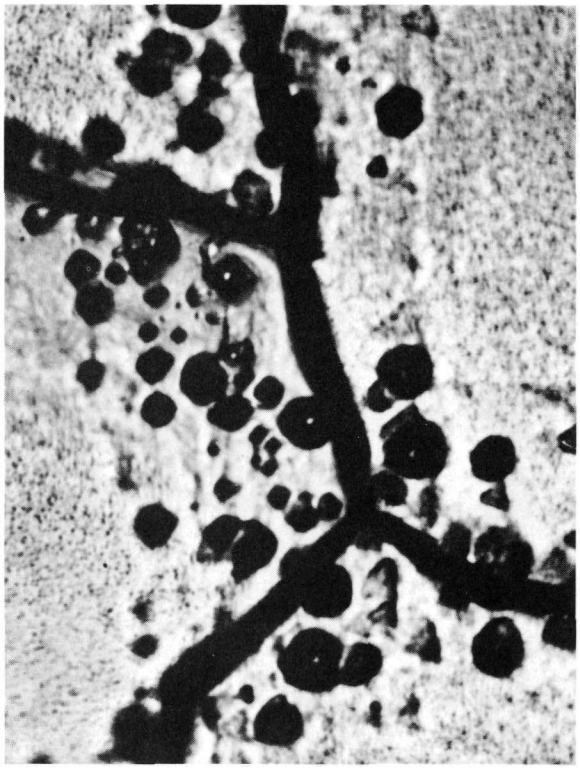

110182 X1000

Figure 1. Aluminum surface after 3-min corrosion in water at 250° C.

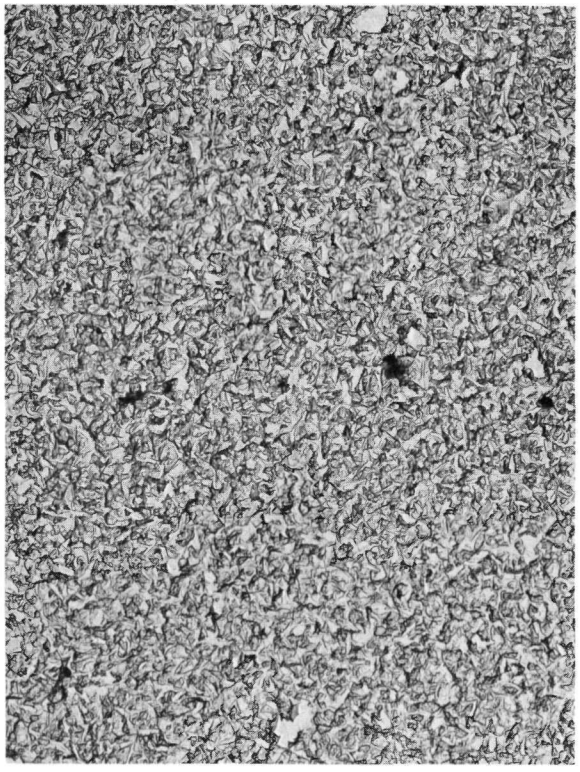

100121 X6000

Figure 2. Carbon replica, preshadowed with Pt-Pd, of aluminum corroded for 4 min at 250° C.

For immersion times longer than 12 minutes, samples were coated with an opaque film which completely hid details on the metal surface.

Observations made in silhouette on drilled discs showed the outer surface to have a "saw-tooth" topography as shown in Fig. 3(a). The surface roughness* of these films remained virtually constant at 2 μ after approximately 4-min corrosion. Surfaces of corroded aluminum were relatively free of growth outcrops; of the samples investigated, only two outcrops were observed. These were opaque to electrons and chunky in appearance, extending 5 μ out from the surface. However, three filamentary outcrops or whiskers were observed on one sample. Two of these were 9 μ long with a length -to-diameter ratio (L/D) of 24, whereas the third, which is shown in part in Fig. 3(a), had a L/D ratio of 75. Fig. 3(b) is a selected area diffraction pattern of the whisker shown in Fig 3(a); it was found to be boehmite (α-$Al_2O_3 \cdot H_2O$). The layer lines in Fig. 3(b) are in a direction normal to the long axis of the whisker, namely, the c direction. This pattern also shows that the crystal has suffered rotational disorientation around the c axis. This is also evident from the diffraction contrast shown in the electron micrograph [see Fig. 3(a)]. No rotation was observed in the diffraction pattern from the two shorter whiskers.

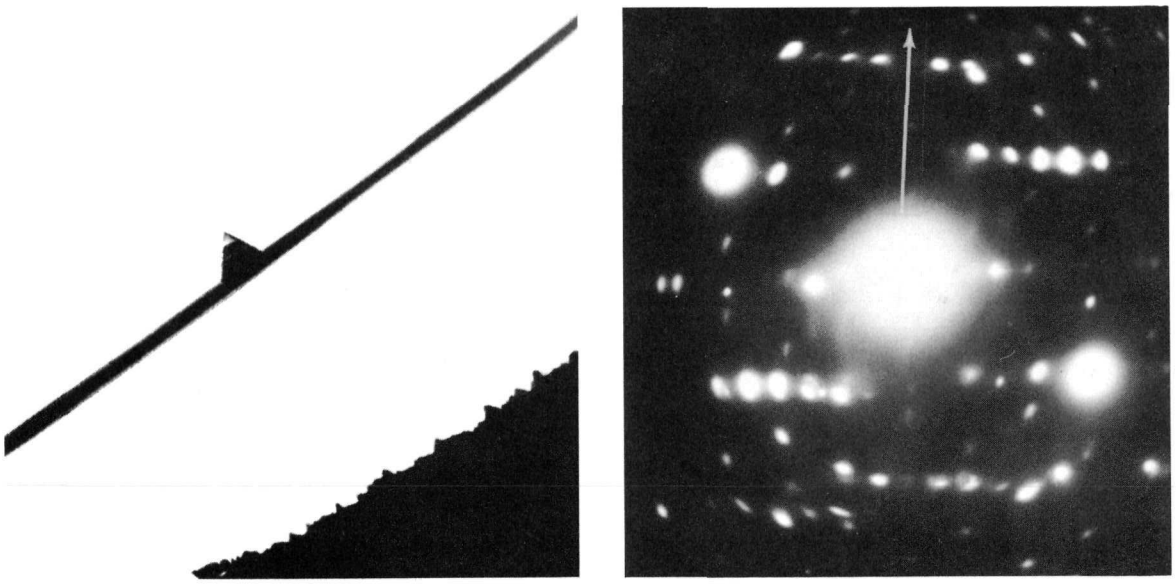

100378 (a) X6000 100379 (b)

Figure 3. (a) Surface topography and whisker on aluminum corroded for 10 min at 250° C. (b) Electron diffraction pattern from whisker shown in (a).

* "roughness" refers to the difference in height between troughs and asperities of the film.

2. A255 Alloy

Figure 4 is a typical example of the second-phase distribution in A255 alloy. Comparison of Fig. 5 with Fig. 4 indicates that the black compound formed from $NiAl_3$ is continuous on the eutectic areas. With increasing exposure, what appears to be a black deposit characteristically spreads across the surface. It has not been possible to choose between a few alternative explanations for the black appearance.

110158 X1000

Figure 4.

Structure of A255 alloy

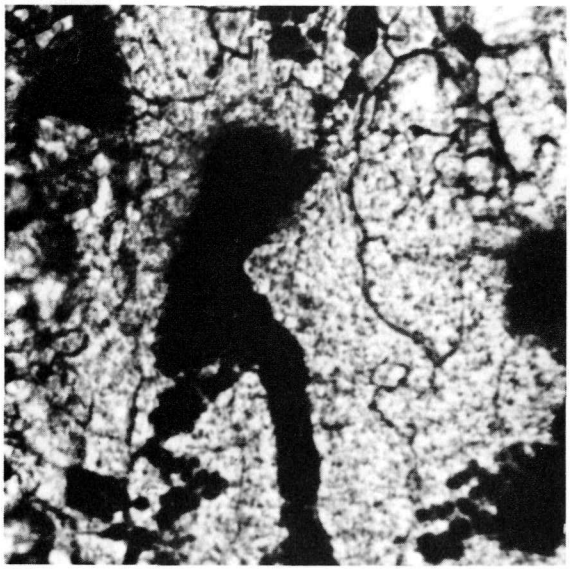

110180 (a) X1000

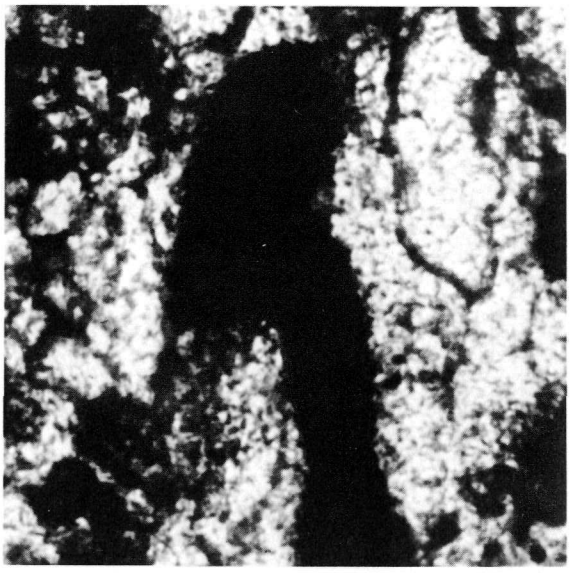

110193 (b) X1000

Figure 5. (a) Precipitate in A255 alloy surface after 3-min corrosion at 250°C. (b) Same area as shown in (a) after 200-min corrosion.

Two-stage preshadowed carbon replicas from the corroded alloy surfaces (less than 12-min immersion) showed that the particle size of the oxide was not uniform and appeared to be controlled by the underlying metal structure. For instance, Fig. 6 shows that the particle size of film over a grain boundary was significantly smaller than over metal grains.

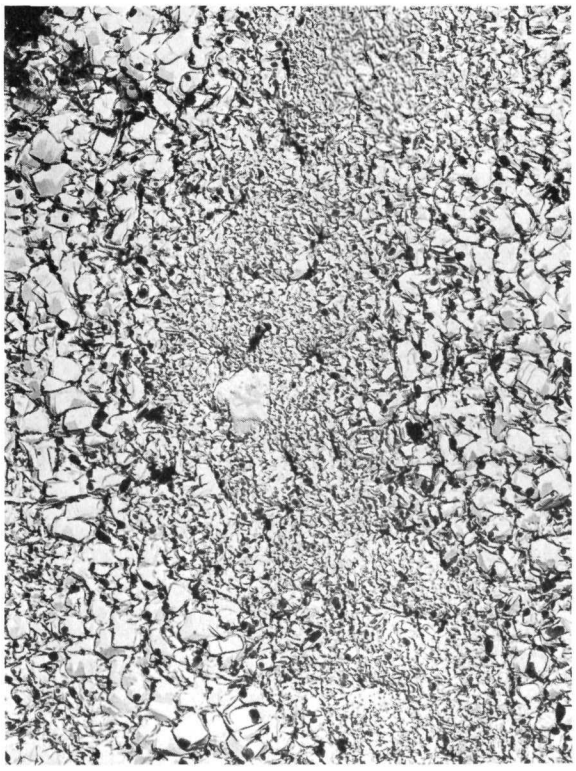

100142 X6000

Figure 6

Carbon replica, preshadowed with Pt-Pd, of A255 alloy after corrosion for 12 min. at 250°C.

Also, one often observed oxide crystals of much larger dimensions, as is shown in Fig. 7 and Fig. 8. Both of these figures were obtained from replicas taken after 12-min corrosion. The black areas in Fig. 8 are oxide outcrops which were extracted from the surface with the plastic impression. Such outcrops appear to be located at the junction in the film between grains of different size. A selected area diffraction examination was done on these particles and they were found to be boehmite.

Examination of disc specimens showed the general surface to be less evenly corroded than the high-purity aluminum; it contained many oxide outcrops which were reasonably closely spaced around the periphery (see Fig. 9). On discs that had been corroded for 200 minutes, boehmite "whiskers" were observed in addition to the other outcrops. Data on whiskers which could be measured with reasonable accuracy are given in Table II.

100141 X16,000

Figure 7. Carbon replica, pre-shadowed with Pt-Pd, of A255 alloy after corrosion for 12 min at 250°C.

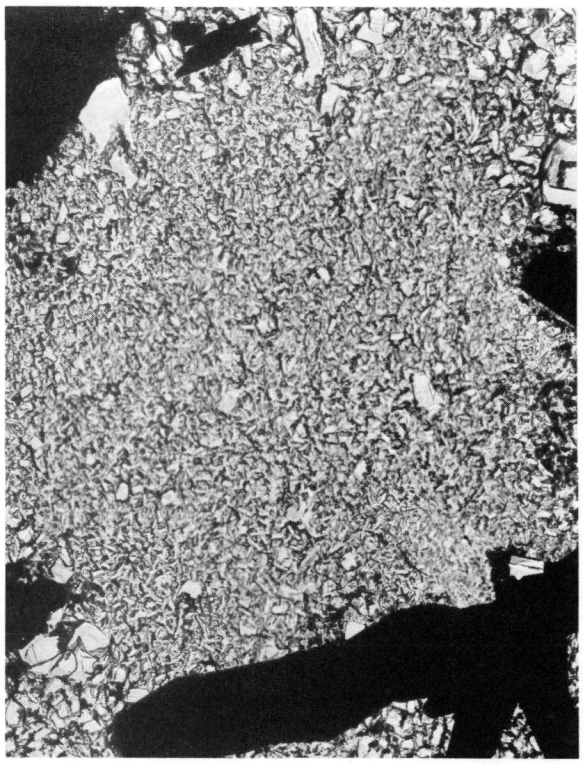

100136 X6000

Figure 8. Carbon replica, pre-shadowed with Pt-Pd, of A255 alloy after corrosion for 12 min at 250°C.

100076 X16,000

Figure 9. Outcropping on A255 alloy disc after corrosion for 4 min at 250°C.

Table II

Whisker Growth on Aluminum at 250°C

Material	Immersion Time, min.	L/D Ratio*	Number of Whiskers Observed
Aluminum	10	24	2
	10	75	1
A255	200	10	6
	200	20	2
	200	30	1
	200	60	1
X8001	5	20	3

* L/D ratio is the ratio of the length of a whisker to its diameter.

Although no whiskers were observed on discs that had been corroded for shorter periods of time, there is a certain amount of evidence from surface replicas that they also grow on short-term specimens.

These whiskers were usually found in clusters, as shown in Fig. 10(a). Selected area diffraction patterns were not obtained from the majority of these because they were too thick to allow electron penetration. In one case, however, a whisker of suitable thickness and sufficiently separated from the rest was obtained. The diffraction pattern of this filament is shown in Fig. 10(b), which indicates that the crystal is boehmite and that the filament axis is parallel to the b-axis of the crystal lattice. This pattern is relative to the (102) plan network of the reciprocal lattice.

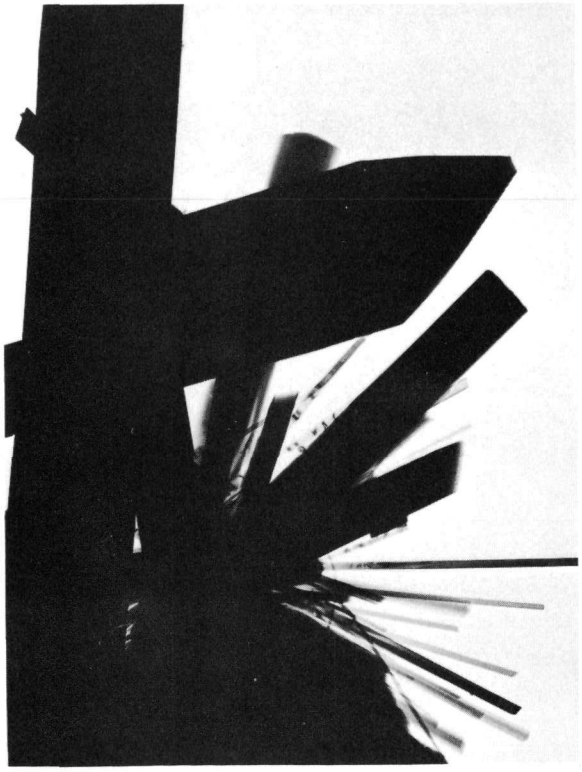

100382 (a) X16,000

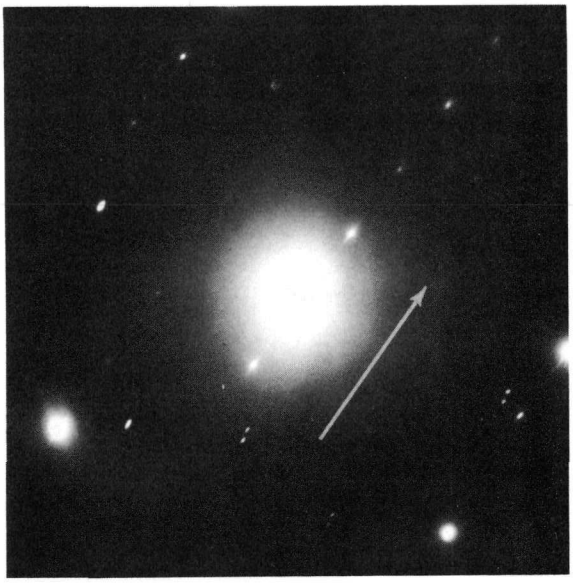

100385 (b)

Figure 10. (a) Whisker growth on A255 alloy after corrosion for 200 min at 250° C.
(b) Diffraction pattern from one of these whiskers.

3. X8001 Alloy

Disc specimens after immersion for 5 minutes showed that the free surface of the corrosion product was slightly smoother than in the case of the A255 alloy. Its topography was still saw-tooth, broken by an occasional outcrop, as shown in Fig. 11. A few whiskers in the grouping L/D = 20 were also observed in electron micrographs.

When the immersion time was increased to 10 minutes, the surface was found to double in roughness and many outcrops, approximately 2 μ in height, were found on scanning the surface. Individual outcrops (Fig. 12) appeared to consist of many small, randomly oriented crystallites. This feature was confirmed by electron diffraction. No whiskers were observed on the 10-minute samples.

100336 X16,000

Figure 11. Outcropping on X8001 alloy disc after corrosion for 5 min at 250°C.

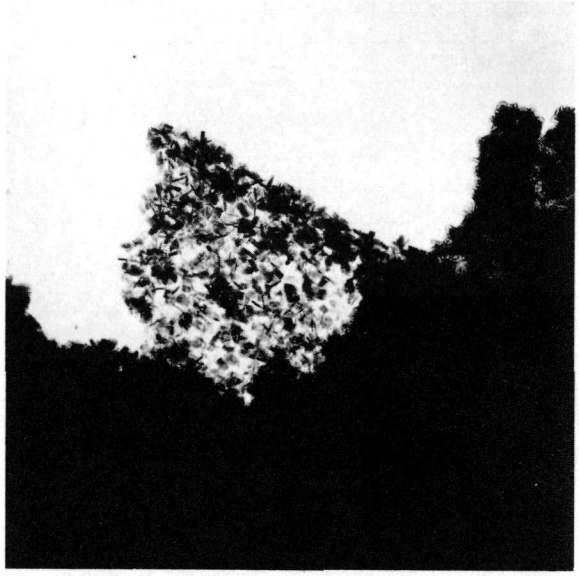

100328 X16,000

Figure 12. Outcropping on X8001 alloy disc after corrosion for 10 min at 250°C.

B. Corrosion at 350°C

1. A255 Alloy

The general surface of disc specimens after the shortest immersion (5 minutes) was saw-tooth in appearance, giving a surface roughness of approximately 0.2 μ. Each asperity was the tip of a small, triangular-shaped platelet, as shown in Fig. 13(a). The angles at these tips

were measured at either 76° or 104°. Some outcrops were observed varying from 1 μ to 4 μ in size.

When immersion was extended to 10 minutes, a surface more densely populated with triangular-shaped platelets was found. Such a surface is shown in Fig. 13(b), which also shows several whiskers. A high-magnification electron micrograph of one platelet is shown in Fig. 14. This figure shows most of the detail that is seen in these thin oxide platelets. The micrograph clearly shows that the structure within each platelet is far from homogeneous. Many areas show elastic bending, resulting in diffraction contrast together with moiré patterns straddling these extinction contours. The cause of these effects is uncertain, but they have been seen to move when thermally excited by the electron beam. Their shape suggests that they may constitute pockets of entrapped gas or liquid which is expelled on heating. Along the outer edge of this crystal a number of mounds can be seen; these appear to be associated with black dots a little way below the surface. It has been suggested that these are nucleation centers for which further growth takes place. In fact, oxide platelets on corroded zirconium (private communication from R. D. Misch) have been found which display additional oxide growth originating at similar spots near the outer surface.

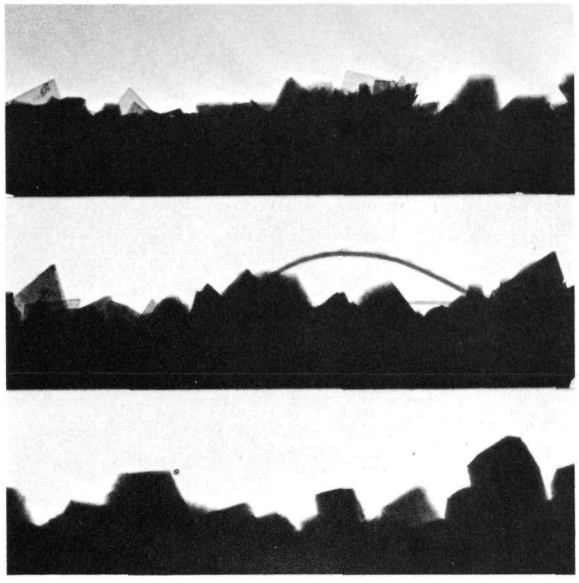

100164

100179

100473

X16,000

Figure 13.

(a) Surface of A255 alloy after 5 min at 350°C.

(b) Surface of A255 alloy after 10 min at 350°C.

(c) Surface of X8001 alloy after corrosion for 200 min at 350°C.

It is quite possible that these "nucleation centers" are small metallic particles which have been transported outwards by the growing oxide. An example of outcropping which was prevalent on specimens corroded for 10 minutes or longer is shown in Fig. 15(a). Selected area diffraction patterns similar to Fig. 15(b) were obtained from these surfaces, showing the material to be boehmite.

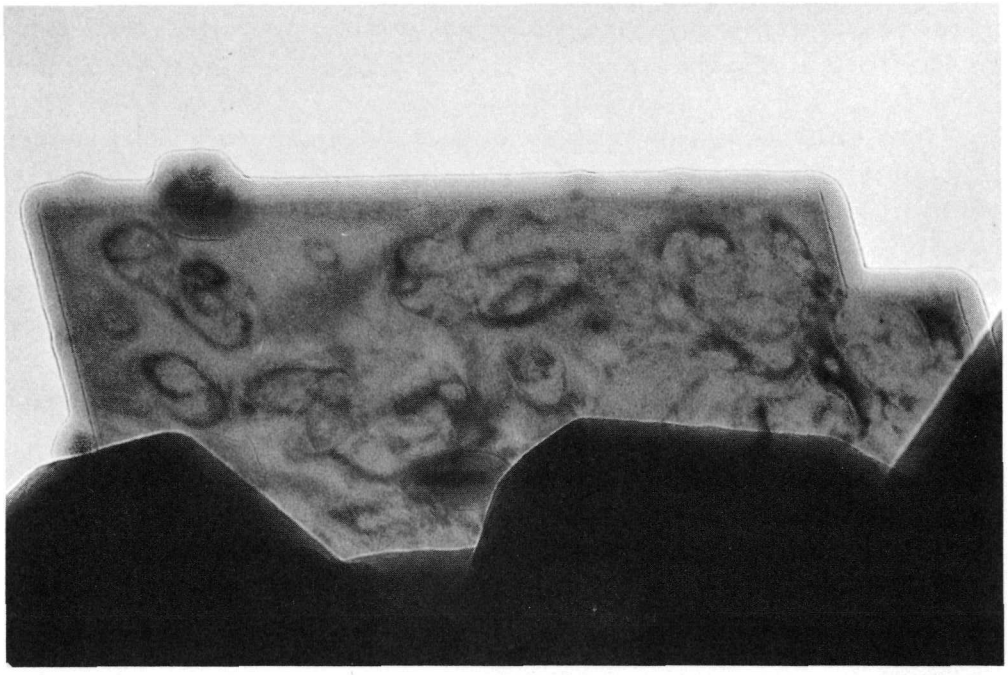

100190 X120,000

Figure 14. Oxide platelet on A255 alloy disc after corrosion for 10 min at 350°C.

Examination of discs in silhouette after corrosion for 24 hours showed the outer surface to be composed of thick oxide blocks, similar to those shown in Fig. 13(c). Outcrops of triangular-shaped platelets, as well as whiskers, were also observed. Some whiskers appeared singly, whereas others were in clusters. Data on these whiskers are given in Table III. A good example of whisker growth is given in Fig. 16.

The morphology of oxide layers on both A255 and X8001 discs after 24-hour to 32-day tests was also investigated optically in transverse section. Several interesting features of film growth were noted. Figure 17 shows the well-crystallized particles which form the outer layer and the "glassy" inner layer (dark in the photograph). The inner layer is not continuous, although when viewed under certain experimental conditions it may appear so. In fact this layer consists of blocks of oxide separated by "cracks." Many of these "cracks" can be traced from the metal to the free surface. Where these conditions exist, whiskers are quite often observed on the free surface.

The ratio of the thickness of the outer crystalline layer to that of the "glassy" inner layer remains substantially constant for corrosion times ranging from 24 hours to 32 days. This ratio of outer to inner film is 1:3. When localized attack of the metal occurs, the outer crystallized

layer increases in thickness immediately above this region. The ratio of the increased depth of penetration into the metal to excess buildup of crystalline product is about 1:1. Over the remainder of the surface the outer to inner oxide ratio remains at 1:3. Figure 18 shows a view of stripped oxide in silhouette where surface outcropping was associated with accelerated attack of the metal.

100177 (a) X16,000

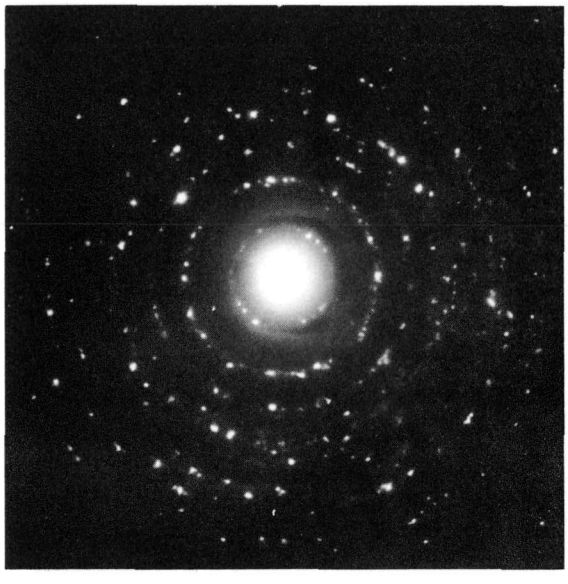

100565 (b)

Figure 15.

(a) Outcropping on A255 alloy disc after corrosion for 10 min at 350° C. (b) Diffraction pattern from the surface.

Table III

Whisker Growth on Aluminum at 350°C

Material	Immersion Time	L/D Ratio	Number of Whiskers Observed
A255	10 min	20	3
	24 hr	10	3
	24 hr	20	1
	24 hr	150	2
X8001	10 min	20	2
	200 min	20	8

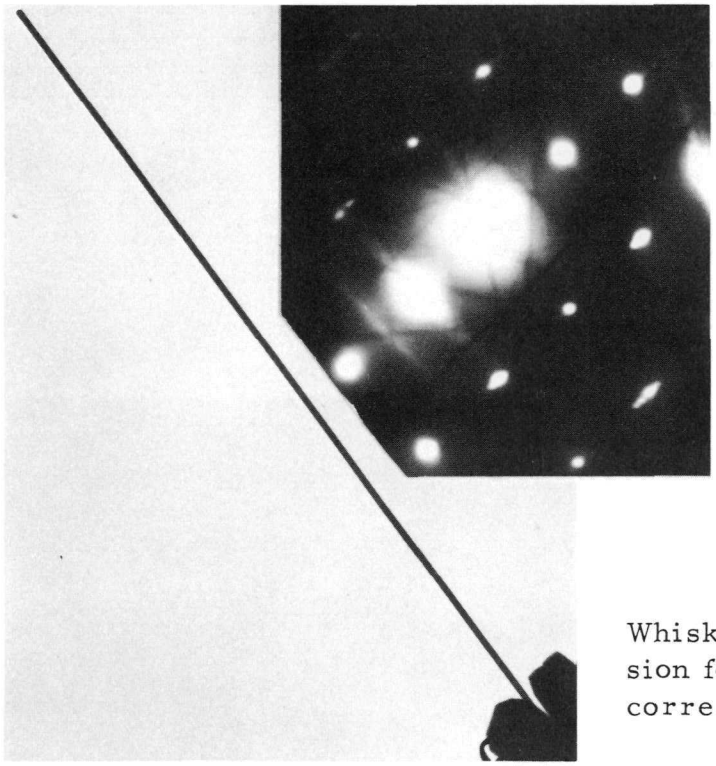

100575 X6000
(inset 100583)

Figure 16.

Whisker on A255 alloy after corrosion for 24 hr at 350°C. Inset is corresponding diffraction pattern.

Some aspects of films produced after 32-day corrosion have been mentioned above. The outer surface was found to contain many clusters of filamentary growth, as well as a considerable quantity of loosely adhering flocculent material, shown at A in Figs. 19 and 20. The nature of this flocculent material was not positively identified, but it is believed to be some form of alumina gel. The oxide filaments were identified by both electron diffraction and X rays as diaspore, the c-axis direction being parallel to the major filament axis. This growth habit for diaspore has previously been reported by Ervin and Osborn.(9)

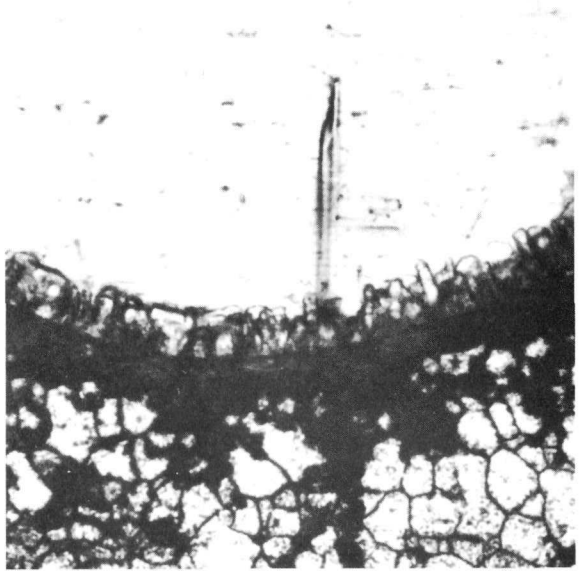

110265 X500

Figure 17. Transverse section of an A255 alloy disc after corrosion for 32 days at 350°C.

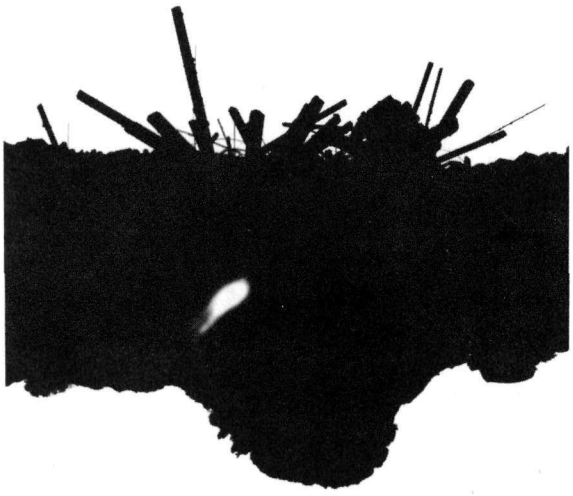

100637 X500

Figure 18. Electron silhouette of oxide layer stripped from A255 alloy disc after corrosion for 32 days at 350°C.

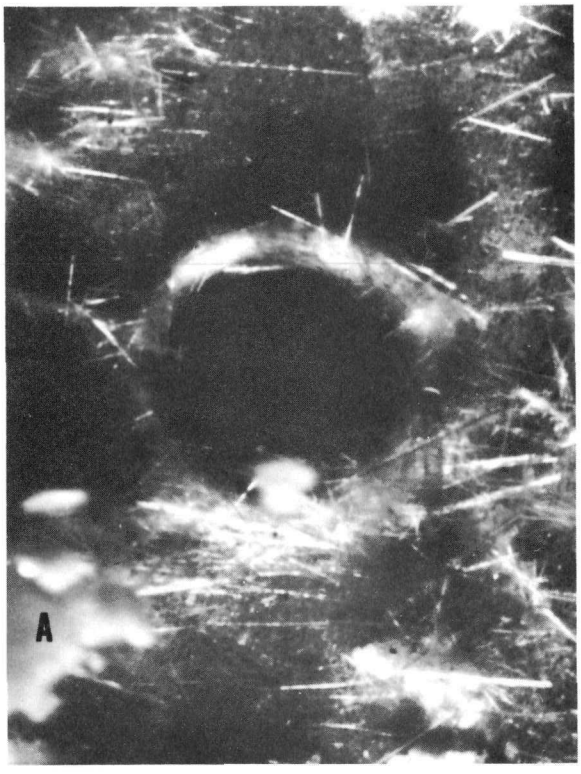

110212 X150

Figure 19.

Optical micrograph of an A255 alloy disc after corrosion for 32 days at 350°C.

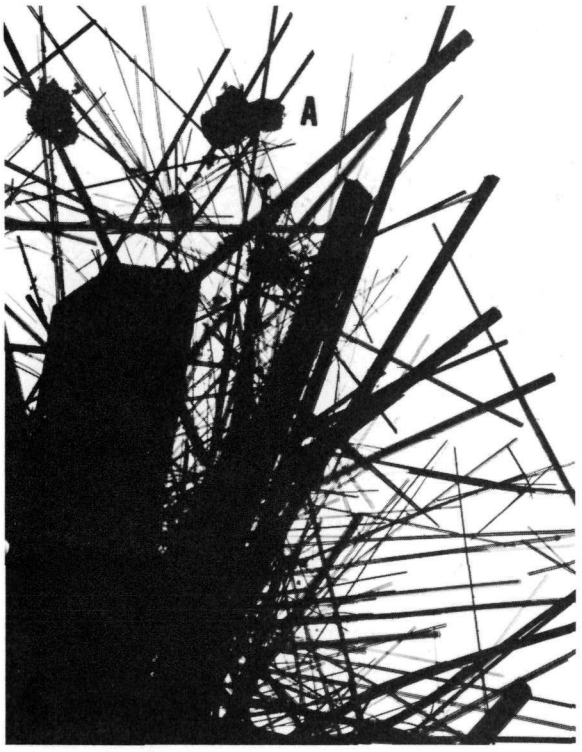

100346 X6000

Figure 20. Electron silhouette of diaspore needles protruding into the hole of the disc shown in Fig. 19.

The appearance of Kikuchi lines as well as of Laue spots on electron diffraction patterns was evidence that the structure of these filaments was highly perfect. Many of these filaments were quite loose and not adherent to the surface oxide at all. They could be easily removed on a needle point. The cross section was found to be rectangular in shape.

2. X8001 Alloy

When viewed in silhouette after corrosion for 5 minutes, the surface of X8001 alloy displayed a similar saw-tooth topography, although slightly rougher than the A255 alloy. Outcropping, some 4-5μ in height, is shown in Fig. 21. After only 10-minute corrosion the surface asperities had thickened considerably and become block type in profile. One transparent platelet was observed, and this showed interesting structural detail. A highly magnified section of this platelet is shown in Fig. 22. Shown in this figure are numerous small loop features varying from 150 Å to 550 Å across. Features of similar appearance to these have been reported by Bassett, Menter and Pashley[10] in single-crystal gold films. It was first thought that they were disloation loops, but this idea was later discredited, since further experiments showed that they appear as a result of electron bombardment; Bassett et al., have considered the possibility that the dot-like features could be associated with the aggregation of gas and/or vacancies in the film, the electron beam being the agent which dissociates the impurity molecules and so effects their ability to diffuse, perhaps in association with a vacancy.

These loop features in Fig. 22 did to a certain extent become mobile under more intensive electron irradiation, with the result that the area shown in this figure appeared to act as a sink for them. It is tentatively suggested that these features may arise from the entrapment of either gas or water during film growth.

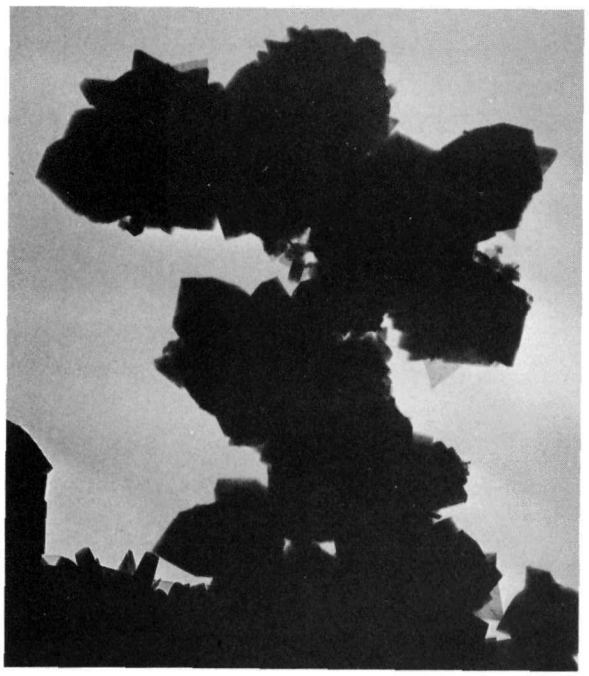

100283 X16,000

Figure 21.

Outcropping on X8001 alloy disc after corrosion for 5 min at 350°C.

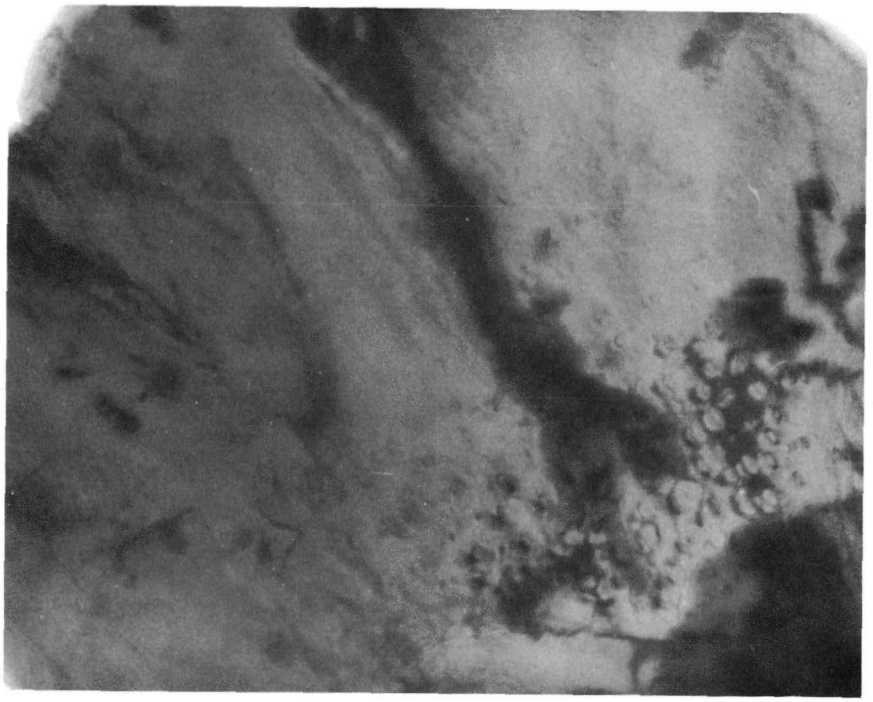

100296 X80,000

Figure 22. Oxide platelet on X8001 alloy disc after corrosion for 10 min at 350°C, showing "loops."

Unfortunately, this specimen was destroyed by the electron beam before it could be determined whether or not these "loops" could be made to conglomerate under electron irradiation.

Several whiskers in the L/D = 20 range were also observed on 10-minute specimens.

After the corrosion time had been extended to 200 minutes, the oxide surface was found to consist mainly of oxide blocks [see Fig. 13(c)] which were opaque to the electron beam. The occurrence of chunky outcrops was very rare but eight whiskers were measured in the L/D = 20 range.

After 24 hours the profile of the outer oxide surface was similar to that recorded for specimens which had been examined after 200-minute corrosion. All the surfaces examined were free of large outcrops and no whiskers were observed. Electron diffraction examination was run on samples of this oxide after it had been gently scraped from the specimen onto a carbon support film. One such particle is shown in Fig. 23(a) and the corresponding diffraction pattern in Fig. 23(b). This pattern corresponds to boehmite and the particle is oriented with the b-axis beam.

Observations made on specimens after 32-day corrosion were similar to those already reported for A255 alloy specimens.

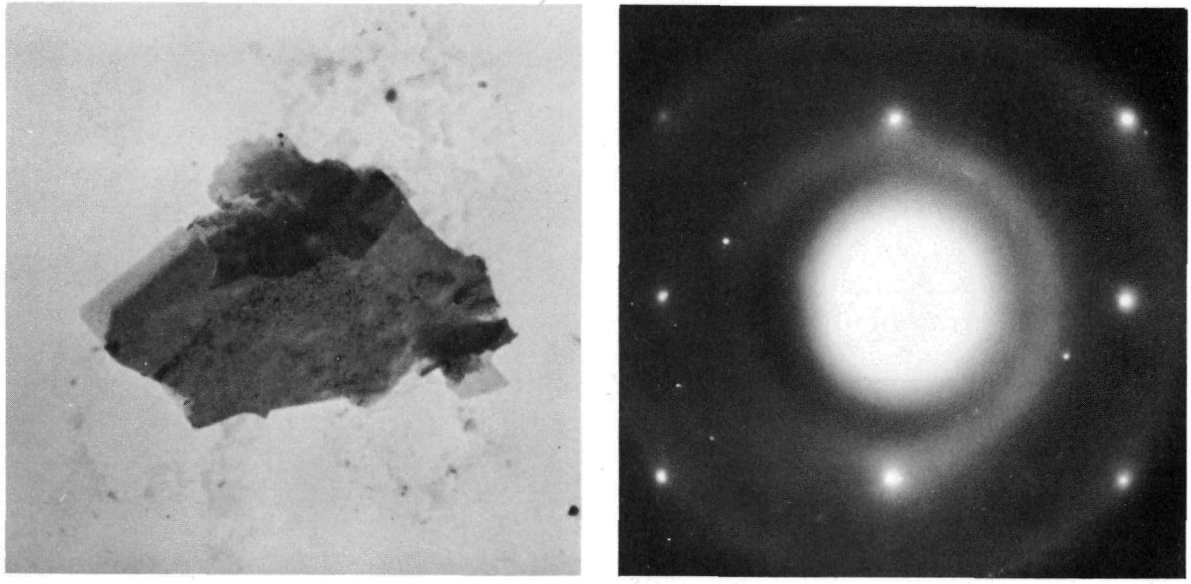

100647 (a) X20,000 100645 (b)

Figure 23. (a) Oxide particle removed from X8001 alloy disc after corrosion for 24 hr at 350°C. (b) Electron diffraction pattern from particle shown in (a).

DISCUSSION

When aluminum and aluminum-nickel alloys are corroded in water at high temperatures, the corrosion products built up on the surface appear in a number of different forms. The present study shows that oxide growth does not advance on a uniform front, but, to the contrary, the advancing surface has been found to contain many outcrops which assume various forms. With the materials investigated these outcrops were thin platelets, chunky outcrops, and whiskers.

In addition to outcrops on the surface, sectioning has shown that the bulk form of these films is not homogeneous. Typically, the metal carries two distinct layers of film material, the inner layer being of small crystal size and "glassy" in appearance, whereas the outer layer consists of well-developed crystallites which appear to prefer growth in the outward direction.

These growth processes suggest that more than one type of crystallization mechanism is operative during film buildup. The general buildup of film on the metal surface by direct reaction between the metal and the corrosive environment can be classified as the primary crystallization process. In this primary process the influence of the metal itself is all important, and its immediate presence at the seat of reaction will directly influence film growth.

The formation of outcrops and the various other growth forms which have been observed can be considered as due to a secondary crystallization process. A good example of secondary crystallization is the formation of diaspore needles on the outer surface of the boehmite film. The experimental evidence suggests that the diaspore crystallizes from solution. Work of Dillon[11] has shown that the solubility of aluminum corrosion product (as Al_2O_3 in g/L) in water at 250°C and 350°C is 1.9×10^{-4} and 2.8×10^{-4}, respectively. Thus it is to be expected that there are sufficient aluminum ions in solution immediately adjacent to the outer oxide surface to allow supersaturation to occur, with the resultant crystallizing out of diaspore. Providing this whole process takes place in the immediate vicinity of the surface, very little matter will be carried away from the surface, even in replenished systems, because of the general flow pattern of liquids over surfaces. Another process not to be overlooked is the crystallization of diaspore from alumina gel.

The experimental conditions used when diaspore was observed are in agreement with the equilibrium diagram for the $Al_2O_3 \cdot H_2O$ system given by Ervin and Osborn.[9]

Although the growth of oxide whiskers has been reported numerous times over the past few years, detailed explanation of their origin is still lacking. Because the rate is much more rapid than that for "normal" oxide,

their growth process must involve a mechanism having an abnormally low activation energy. This could come about through some combination of a decrease in the energy level of the activation complex and through a high local energy. The latter has received somewhat more consideration. Evidence to date appears to support the theory that whiskers grow from highly imperfect material. Also, whisker growth has been associated with pressure, which can accelerate growth by as much as 10,000. The tendency for more whiskers to be produced at the higher temperature may have been influenced by pressure (2400 psi in the present investigation). However, it is difficult to visualize how suitable experiments could be performed under the present experimental conditions to ascertain the role of pressure in the production of oxide whiskers.

Yet another reason for whisker growth on corroding aluminum surfaces may be anisotropic thermal stresses and/or those derived from misfit between metal and growing oxide.

Experimental evidence has been presented here to show that whiskers, as well as the other forms of outcrops, grow out from what is essentially a "semiporous" substrate, i.e., the general oxide film. From this substrate their growth is in one of several preferred directions, and the whiskers are essentially regular in cross section. Whether they grow from the base or the tip has not been established, and also no direct evidence has been obtained to show that these whiskers are in any way associated with dislocations.

ACKNOWLEDGEMENTS

The author wishes to thank D. Dorman and M. J. Heyduk for preparing the samples and corroding them. The discussions with J. E. Draley during the course of this work were also much appreciated.

REFERENCES

1. Halliday, J. S. and Hirst, W., Proc. Phys. Soc., 68, 178 (1955).

2. Brenner, S. S., Acta Met., 4, 62 (1956).

3. Nabarro, F. R. N. and Jackson, P. J., Proceedings of an International Conference on Crystal Growth, Cooperstown, New York (1958), p. 13.

4. Wislicenus, H., Kolloid-Zeits., 100, 66 (1942).

5. Webb, W. W., Dragsdorf, R. D., and Forgeng, W. D., Phys. Rev., 108, 498 (1957).

6. Webb, W. W. and Forgeng, W. D., J. Appl. Phys., 28, 1449 (1957).

7. Pryor, M. J. and Keir, D. S., J. Electrochem. Soc., 102, 370 (1955).

8. Draley, J. E. and Ruther, W., Corrosion, 12, 20 (1956).

9. Ervin, G., and Osborn, E. F., J. Geol., 59, 381 (1951).

10. Bassett, G. A., Menter, J. W., and Pashley, D. W., Proc. Inter. Conf. on Structure and Properties of Thin Films, Bolton Landing, John Wiley and Sons, New York, September, 1959, p. 11.

11. Dillon, R. L., Dissolution of Aluminum Oxide as a Regulating Factor in Aqueous Aluminum Corrosion, HW-61089 (August 1959).

12. Fisher, R. M., Darken, L. S. and Carroll, K. G., Acta Met., 2, 368 (1954).